Contents lists available at ScienceDirect

Toxicology Reports

Oxidative damage and cell cycle delay induced by vanadium(III) in human peripheral blood cells

V.A. Alcántara-Mejía [a,d], J.J. Rodríguez-Mercado [a,*], R.A. Mateos-Nava [a], L. Álvarez-Barrera [a], E. Santiago-Osorio [b], E. Bonilla-González [c], M.A. Altamirano-Lozano [a]

[a] Unidad de Investigación en Genética y Toxicología Ambiental, Unidad Multidisciplinaria de Investigación Experimental (UMIE-Z), Facultad de Estudios Superiores-Zaragoza, Campus II, UNAM, Ciudad de México 09230, Mexico
[b] Unidad de Investigación en Diferenciación Celular y Cáncer, UMIE-Z, Facultad de Estudios Superiores-Zaragoza, Campus II, UNAM, Ciudad de México 09230, Mexico
[c] Departamento de Ciencias de la Salud, Universidad Autónoma Metropolitana-Campus Iztapalapa, Ciudad de México 09340, Mexico
[d] Posgrado en Ciencias Biológicas, UNAM, Edificio E, Primer Piso, Circuito de Posgrados, Ciudad Universitaria, Coyoacán, Ciudad de México 04510, Mexico

ARTICLE INFO

ABSTRACT

Vanadium (V) is a metal that can enter the environment through natural routes or anthropogenic activity. In the atmosphere, V is present as V oxides, among which vanadium(III) oxide (V_2O_3) stands out. Cytogenetic studies have shown that V_2O_3 is genotoxic and cytostatic and induces DNA damage; however, the molecular mechanisms leading to these effects have not been fully explored. Therefore, we treated human peripheral blood lymphocytes *in vitro*, evaluated the effects of V_2O_3 on the phases of the cell cycle and the expression of molecules that control the cell cycle and examined DNA damage and the induction of oxidative stress. The results revealed that V_2O_3 did not affect cell viability at the different concentrations (2, 4, 8 or 16 μg/mL) or exposure times (24 h) used. However, V_2O_3 affected the percentage of G_1- and S-phase cells in the cell cycle, decreased the expression of mRNAs encoding related proteins (cyclin D, cyclin E, CDK2 and CDK4) and increased the expression of γH2AX and the levels of reactive oxygen species. The ability of V_2O_3 to cause a cell cycle delay in G_1-S phase may be associated with a decrease in the mRNA and protein expression of the cyclins/CDKs and with intracellular oxidative stress, which may cause DNA double-strand damage and H2AX phosphorylation.

1. Introduction

Vanadium (V) is a transition metal found in nature in approximately 65 minerals; it ranks fifth among the most abundant metals in the Earth's crust and first in the ocean [1]. V has various oxidation states, and its +3, +4, and +5 oxides are an environmental problem. It is estimated that 130,000 to 260,000 tons of V are released per year, including approximately 65,000 tons from forest fires, volcanic eruptions and mineral erosion; the remainder of V is of anthropogenic origin [2]. The main sources of emissions are the burning of fossil fuels, metallurgical mining, chemical, agricultural, energy and other industrial activities [1,3,4]. The chemical species released into the environment include vanadium oxides, among which vanadium(V) oxide, a pentoxide, is the most abundant (V_2O_5), followed by oxides in oxidation states IV and III (V_2O_4 and V_2O_3, respectively) [5,6]. In recent years, some companies have attempted to reduce V_2O_5 emissions, as V_2O_5 is corrosive to the metal parts of machinery and causes other oxides to be

released (such as V_2O_3) by manufacturing catalysts that prevent the formation of V_2O_5 [7,8]. The effects of occupational and environmental exposure to V are well documented, and environmental exposure can cause respiratory distress, organ damage, and possibly death [9,10].

Previous studies have investigated the *in vitro* and *in vivo* effects of vanadium oxides. In animals, exposure to 1.56 mg/m³ V_2O_5 via inhalation caused neuronal death in Wistar rats, whereas 0.02 M V_2O_5 in CD-1 mice led to hyperplasia of the bronchiolar epithelium, small inflammatory foci, and sloughing of nonciliated bronchiolar cells. Additionally, intraperitoneal administration of 4.7, 9.4, or 18.7 mg/kg V_2O_3 induced chromosomal aberrations and altered cell division in the bone marrow cells of CD-1 mice, as well as in Chinese hamster ovary cells (24.9 μg/mL) [11–17]. However, the degree of toxicity depends on the oxidation state of the metal, with each oxide exerting its own effects. Cytogenetic assays revealed that V_2O_3 is cytotoxic and genotoxic in leukocytes and lymphocytes (1–16 μg/mL). Metal decreases the mitotic index and the cell proliferation index, increases premature centromere

Table 1

Primer sequence. A reference gene (GAPDH) was used to evaluate the expression of *P53, P21, CYCLIN D, CYCLIN E, CDK2* and *CDK4*.

Gen	Forward	Reverse	pb
GAPDH	5´GGAGCGAGATCCCTCCAAAAT 3´	5´GGCTGTTGTCATACTTCTCATGG 3´	197
P53	5´CTGGCCCCTGTCATCTTCTG 3´	5´CCGTCATGTGCTGTGACTGC 3´	242
P21	5´TGAGCGATGGAACTTCGACT 3´	5´GACAGTGACAGGTCCACATGG 3´	210
CICLINA D	5´TACTTCAAGTGCGTGCAGAAGGAC 3´	5´TCCCACACTTCCAGTTGCGATCAT 3´	498
CICLINA E	5´TCCTGGATGTTGACTGCCTT 3´	5´CACCACTGATACCCTGAAACCT 3´	109
CDK 2	5´CCTGGATGAAGATGGACGGA 3´	5´TGGAAGAAAGGGTGAGCCA 3´	99
CDK 4	5´CAGATGGCACTTACACCCGT 3´	5´GTTTCCACAGAAGAGAGGCTTTC 3´	150

The genes were purchased from Alpha DNA, PROBIOTEK.

Table 2

Viability of human lymphocyte cultures before treatment (0 h) and 24 h after exposure to V_2O_3.

V_2O_3 treatment in µg/mL	Viability (%)	
	0 h	24 h
0 (without)	99.5 ± 0.5	97.7 ± 2.6
2	98.7 ± 1.5	95.5 ± 4.7
4	99.1 ± 0.5	95.5 ± 1.9
8	99.0 ± 0.8	96.2 ± 1.7
16	98.5 ± 1.7	97.0 ± 3.4

Data are presented as the mean ± SD, from three independent experiments performed in duplicate (n = 6).

separation and produces single-strand breaks in DNA [16–20]. The results of chromosomal damage are inconclusive; *in vivo* structural chromosomal aberrations are increased [16,19], but this effect is not observed in human leukocyte and lymphocyte cultures [16–20].

DNA damage is known to activate several cellular responses through complex protein networks, including cell cycle control and DNA repair proteins [21]. Single- and double-strand breaks in DNA are detected by proteins such as ataxia-telangiectasia mutated Rad3-related (ATR) and ataxia-telangiectasia mutated (ATM); both signaling pathways converge on the phosphorylation of histone H2AX [22,23], and H2AX expression provides an indicator of DNA damage due to xenobiotic exposure [22, 24,25]. γH2AX recruits Brca1 and 53BP1 (p53) [26,27], the latter of which is responsible for cell cycle sensing, to repair DNA damage (cell survival) or to activate cell death signals, such as those for apoptosis [28]. V_2O_3 induces genotoxicity; however, DNA damage sensor proteins, such as p53, do not change (2–16 µg/mL) in human lymphocyte cultures [12], so damage may be sensed by other proteins, such as γH2AX. Therefore, in the present study, we focused on the effects of vanadium (III) oxide on the cell cycle; the expression of both mRNAs to generate their proteins, which control the cell cycle; the expression of a DNA damage sensor protein (γH2AX); and the assessment of oxidative stress in human peripheral blood cells *in vitro*.

Hence, we investigated whether exposure to this compound induces cell cycle arrest due to decreased mRNA and protein levels triggered by DNA damage through oxidative stress. To achieve this goal, we treated isolated cells with V_2O_3, and the DNA content was determined for analysis of the cell cycle and reactive oxygen species (ROS) production via flow cytometry; moreover, the protein levels of cyclins, and γH2AX were evaluated via Western blotting, and the mRNA expression levels of cyclins and were assessed via PCR. In this way, we helped elucidate the genotoxic and cytostatic mechanism of V_2O_3.

2. Materials and methods

2.1. Reagents

The following reagents were used for the development of the protocols: vanadium(III) oxide (V_2O_3, CAS 1314–34–7 with 99.99 % purity), which was macerated and dissolved in distilled water; Histopaque®-1077; 5(6)-carboxyfluorescein diacetate mixed isomers (CFDA); ethidium bromide (BE); phosphate-buffered saline (PBS); and propidium iodide from Sigma—Aldrich, Inc. (MO, USA). PB-MAXTM Karyotyping Medium was from Gibco BRL-Invitrogen Corporation (NY, USA). Acrylamide, N,N-methylene-bis-acrylamide, glycine, sodium dodecylsulfate (SDS), `N,`N,`N,`N,`N-tetra-methyl-ethylenediamine (TEMED), tris hydroxymethyl-aminomethane (Tris), ammonium persulfate, and the Bio-Rad protein assay mixture were obtained from Bio-Rad Laboratories (CA, USA).

The protease inhibitors aprotinin and leupeptin, the primary antibodies anti-cyclin D (sc-246), anti-cyclin E (sc-248), anti-CDK 2 (sc-6248), anti-CDK 4 (sc-53636), anti-actin (sc-8432), and anti-γH2AX (sc-517348), the horseradish peroxidase-conjugated secondary antibody m-IgGk BP-HRP (sc-516102), the goat anti-mouse IgG-HRP, Tween-20, the Luminol Reagent sc-2048 for western blotting and dihydrorhodamine 123 (sc-203027) were obtained from Santa Cruz Biotechnology, Inc. (CA, USA). Ethylenediaminetetraacetic acid (EDTA) was obtained from BD Diagnostics Mexico. TRIzol Reagent, ReverAid First Strand cDNA (K-1622) and Maxima SYBR Green/ROX qPCR Master Mix (K-0221) were
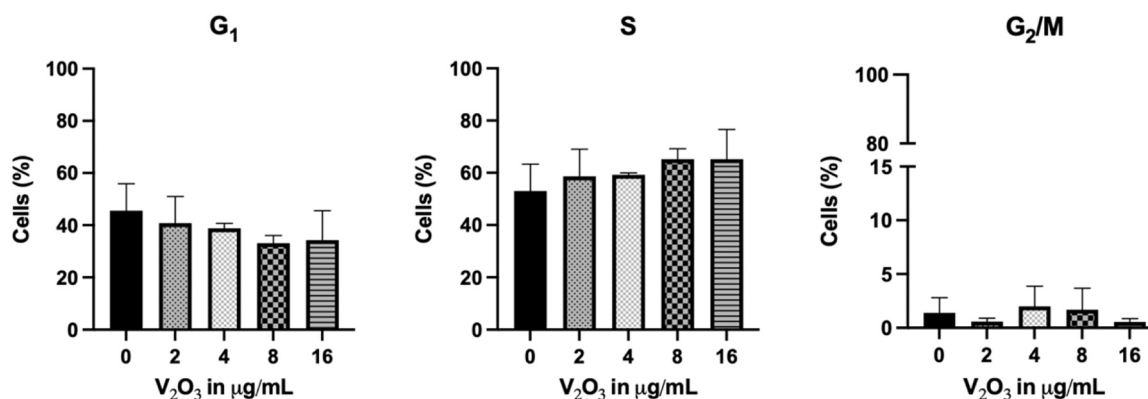

Fig. 1. Estimation of the percentage of cells in G_1, S and G_2/M phase of human lymphocytes treated with 0 (untreated), 2, 4, 6, 8 and 16 µg/mL V_2O_3 for 24 h. Data are presented as the means ± SDs of three independent experiments performed in duplicate (n = 6).
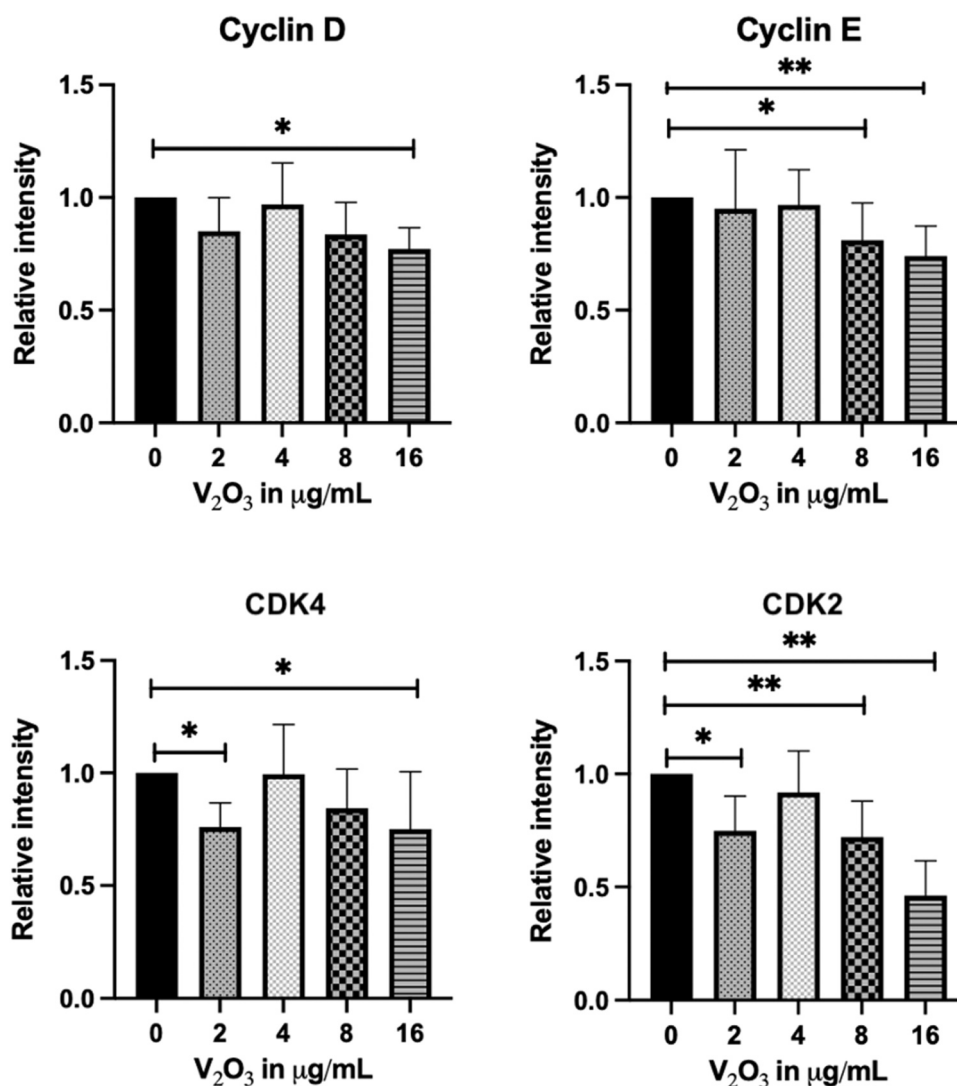
Fig. 2. The relative intensity of cyclin D, cyclin E, CDK4 and CDK2 proteins from human lymphocyte cultures treated with 0 (untreated), 2, 4, 8 and 16 μg/mL V_2O_3 for 24 h. Data are presented as the means $\pm$ SDs to three independent experiments with their duplicates (n = 6). * $p < 0.05$, ** $p < 0.01$ compared to the untreated group (ANOVA-Tukey).

obtained from Thermo Fisher Scientific (MA, USA).

2.2. Lymphocyte cultures and treatments

Peripheral blood samples were collected from three volunteers via the Vacutainer® system. Lymphocytes were isolated with Histopaque®-1077 and incubated at 1×10^7 in 5 mL of culture medium for 48 h at 37 °C. Twenty-four hours after culture initiation, V_2O_3 treatments were administered at concentrations of 2, 4, 8 or 16 μg/mL, and the mixture was incubated for 24 h; an untreated group (0 μg/mL) was established. The concentrations used were selected according to previous reports. To ensure that the added vanadium dissolved in the medium, we assessed all the cell cultures at the end of each test and ensured that there were no particles or precipitates. The procedures involving human volunteers who provided written informed consent were obtained from each blood donor, adhered to the guidelines of the Helsinki and Tokyo Declarations and were approved by the Committee of Ethics and Biosecurity of the FES-Zaragoza, UNAM (registration number FESZ-CE/21–118–01).

2.3. Cell viability

Cell viability was assessed at the beginning and end of the exposure

time to V_2O_3 via dual staining with fluorochromes (0.125 μg/μL CFDA and 0.025 μg/μL BE). Ten microliters of the cell sample was placed in 10 μL of the fluorochrome mixture (1:1) and incubated for 15 min. Subsequently, under a fluorescence microscope (Nikon HFX-DX Opti-phot-2 with Filter G-2A), 100 cells per culture were sorted by separating viable cells (emitting green fluorescence) from nonviable cells (nuclei fluorescing red).

2.4. Cell cycle analysis of DNA content

After 24 h of exposure to V_2O_3, the DNA content in the different phases of the cell cycle was analyzed via flow cytometry. The cells were fixed, permeabilized and incubated in staining solution (0.1 % Triton X-100/PBS, 200 μg/mL RNase A and 50 μg/mL propidium iodide). A total of 1×10^4 cells were acquired on a BD FACSAriaTM II cytometer (Becton Dickinson and Company, CA, USA.) Histograms were constructed via WinMDI 2.9 software developed by Joseph Trotter. The number of nuclei in each phase of the cell cycle (G_1, S and G_2/M) was estimated via the free software Cylchred developed by T. Hoy, Cardiff University.
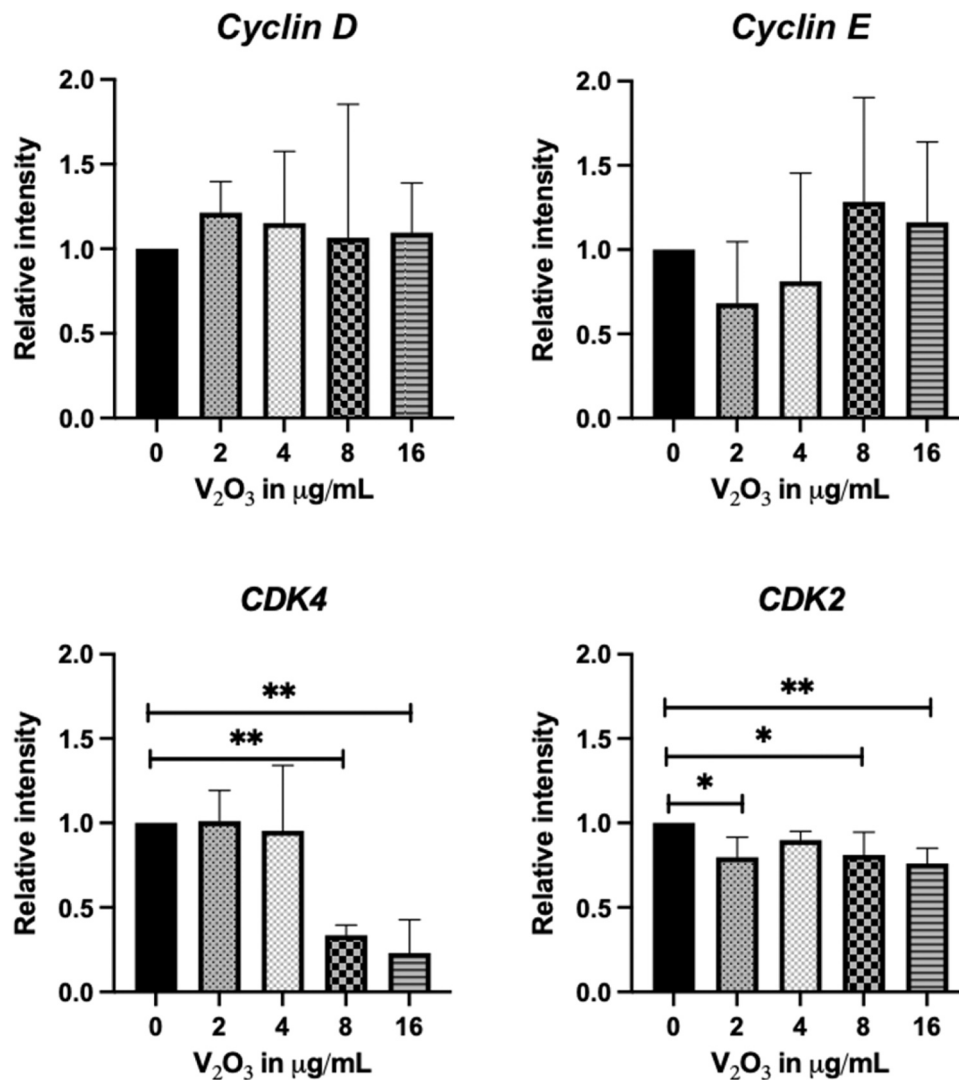
Fig. 3. Relative mRNA intensity of *cyclin D, cyclin E, CDK4* and *CDK2* in human lymphocyte cultures treated with 0 (untreated), 2, 4, 8 and 16 μg/mL V_2O_3 for 24 h. Data are presented as the means ± SDs from three independent experiments with duplicate samples (n = 6). * $p < 0.05$, ** $p < 0.01$ compared to the untreated group (ANOVA-Tukey).

2.5. Analysis of protein expression levels

At the end of the treatments, proteins were obtained by lysing the cells with RIPA buffer (150 mM NaCl, 5 mM EDTA, 1 % Nonidet P-40, 0.1 % SDS, 1 mM DTT, 1 mM $NaVO_4$, 1 mM Na_2HPO_4, 5 mM Na_2HPO_4 and 10 mM NaH_2PO_4) and protease inhibitors. The protein concentration was determined via the use of the Bio-Rad protein assay reagent.

The proteins were subsequently separated via 12 % polyacrylamide gel electrophoresis (SDS—PAGE) by applying a constant current of 100 V, transferred to a Bio-Rad PVDF membrane by electroblotting with a constant current of 145 mA, blocked with 5 % TBST fat-free milk powder (0.05 % Tween 20 in Tris-buffered saline) and then incubated overnight at 4 °C with one of the following primary antibodies: anti-cyclin D, anti-cyclin E, anti-CDK4, anti-CDK2, anti-γH2AX or anti-actin (the latter as a loading marker).

The membrane was incubated with the secondary antibody for 90 min, washed and subsequently incubated with luminol Western reagent. Proteins of interest were visualized as bands. The relative intensity of the proteins was assessed via ImageJ 1.45 software (NIH, USA; available at http://rsb.info.nih.gov/ij).

2.6. RNA extraction and cDNA synthesis

Total RNA was isolated from 1×10^7 cells via the standard TRIzol extraction method and recovered in 40 μL of molecular biology grade water, after which its purity and quantity were determined via a bio-photometer (Eppendorf AG 22331). In addition, the integrity of the total RNA was determined via horizontal agarose gel electrophoresis (1 %).

The RNA samples were reverse transcribed into cDNA in a total volume of 20 μl with 5 μl of total RNA, 1 μl of oligo primer (dT) and a RevertAid First Strand cDNA Synthesis Kit containing 5X reagent buffer, an RNase inhibitor, dNTPs and RevertAid M-MuLV RT, following the supplier's instructions. The reaction was carried out at 42 °C for 60 min and finally for 5 min at 70 °C. The reaction tubes containing the reverse transcription (RT) preparations were subsequently cooled in an ice chamber for PCR amplification of the cDNA.

2.7. Polymerase chain reaction (PCR)

The specific primer sequences and product sizes are listed in Table 1. GAPDH was used as a constitutively expressed gene to normalize the expression levels of the target genes. The reaction mixture for RT—PCR (10 mM dNTPs, 50 mM $MgCl_2$, 10x PCR buffer (50 mM KCl, 20 mM Tris-
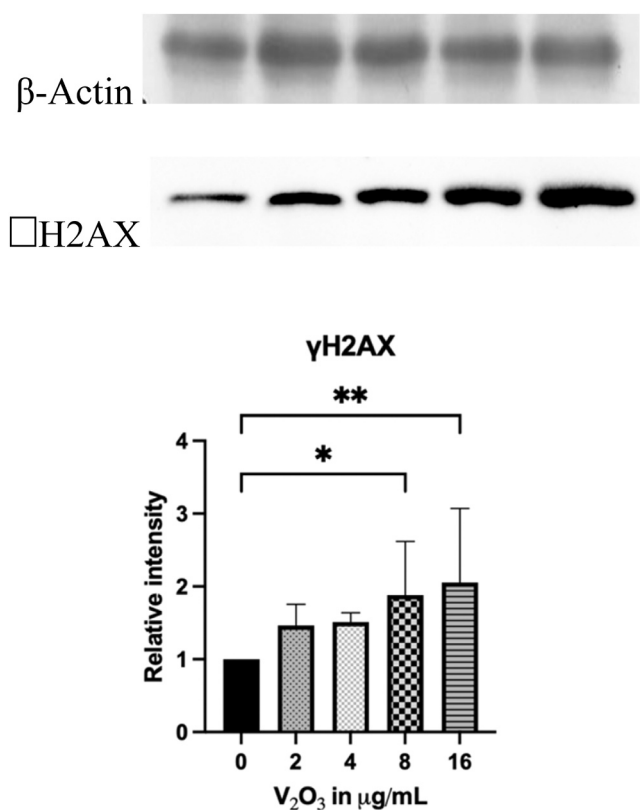
β-Actin

☐H2AX

Fig. 4. Normalized data on the relative intensity of γH2AX (DNA damage sensor) protein from human lymphocyte cultures treated with 0 (untreated), 2, 4, 8 and 16 μg/mL V_2O_3 for 24 h are presented. Data are presented as the means ± SDs of three independent experiments with duplicate samples (n = 6). * p < 0.05, ** p < 0.01 compared to no treatment (ANOVA-Tukey).
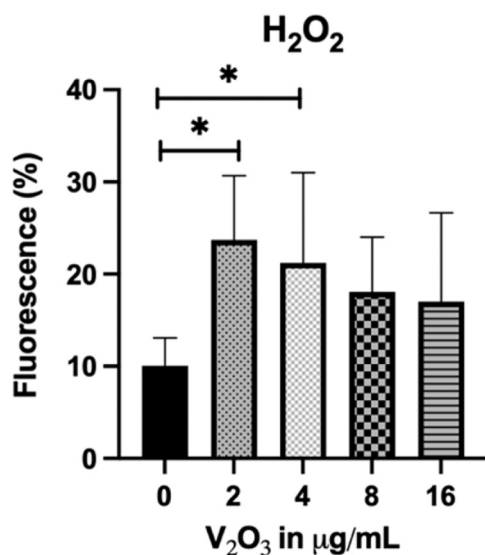

Fig. 5. Estimation of the percentage of cells fluorescing by DHR oxidation in human lymphocytes treated with 0 (untreated), 2, 4, 8 and 16 μg/mL V_2O_3 for 24 h. Data are presented as the means ± SDs of three independent experiments performed in duplicate (n = 6). * p < 0.05 compared to the untreated group (ANOVA-Dunnett).

HCl at pH 8.3) and RNase-free water) was placed in a thermal cycler under the following conditions: 95 °C for 120 s, 95 °C for 15 s, 64 °C for 30 s, and 72 °C for 60 s. The last three steps were repeated for 30 cycles,

followed by a step of 72 °C for 5 min. The PCR products were loaded onto an agarose gel (1 %) together with the GAPDH-derived PCR products from the different samples. With the help of the Bio-Rad program of the ChemiDoc™ kit, the relative intensity of gene expression was obtained.

2.8. Assessment of ROS

Dihydrorhodamine 123 (DHR) dye was used to assess the level of intracellular ROS in the form of hydrogen peroxide (H_2O_2). The cells were incubated with 10 μM DHR for 30 min in the dark at 37 °C, and the excess dye was removed with PBS. Samples were assessed by flow cytometry (BD FACSAria II from BDBiosciences®) to acquire 2×10^4 cells at 505 nm excitation and 529 nm emission, and analyses were performed on a Floreada.io. system (2022) (https://floreada.io/).

2.9. Statistical analyses

The data obtained were analyzed via Prism 9.0.1 software for Mac and are presented as the means ± standard deviations (SDs) of three independent experiments performed in duplicate (n = 6). For identification of the significant differences between the treated and untreated groups, ANOVA was applied with Tukey's (equal variances) or Dunnett's (different variances) *post hoc* test; p < 0.05 or p < 0.01 was considered a significant value.

3. Results and discussion

3.1. Cell viability

An important mechanism of metal toxicity is delivery to the inside of the cell. Substances that are poorly soluble may be absorbed; vanadium compounds can enter through ionic channels, undergo passive diffusion, and undergo endocytosis. Notably, vanadium ions preferentially use receptor-mediated endocytosis by binding to transferrin. Additionally, entry into the cell is not altered by amino acids, phosphate, or other possible vanadium binders present in the cell culture medium [18, 29–32].

The viability test with CFDA-BE is an indicator of metabolic activity and death due to cell membrane damage. The different treatments with V_2O_3 did not affect the viability of lymphocytes (Table 2). In untreated cultures, viability was greater than 97 %, whereas in treated cultures, viability was greater than 95 %. Treatment with V_2O_3 did not change the percentage of viable lymphocytes after 24 h of treatment, and the results correspond with previous reports for this compound [12,20] and for other vanadium oxides [18,33] in human lymphocytes and leukocytes. However, V and its compounds are known to induce cell toxicity at concentrations ≥ 200 μM and exposure times of 48 h or more [34,35].

3.2. Cell cycle

For the analysis of DNA content to determine the different phases of the cell cycle, we observed a trend in which the percentage of cells in the G_1 phase decreased while the proportion of cells in the S phase increased, mainly in cultures treated with 8 and 16 μg/mL V_2O_3. (45.57 ± 9.26 G_1 phase of the control group vs. 33.08 ± 2.98 and 34.27 ± 10.23 at concentrations of 8 and 16 μg/mL vanadium, respectively). Although these results are not statistically significant, we concluded that there is a cell cycle delay in the G_1 to S transition (Fig. 1). Vanadium oxides are cytostatic, as they reduce the proportion of cells entering mitosis and decrease the number of times a cell divides [17,36,37]. Cytogenetic studies of human lymphocyte cultures have shown that V_2O_3 increases the average generation time by 26–32 h [20], indicating disturbances in cell cycle progression. In this study, we detected a decrease in the number of cells in the G_1 phase and an increase in the number of cells in the S phase of the cell cycle. Although our results are
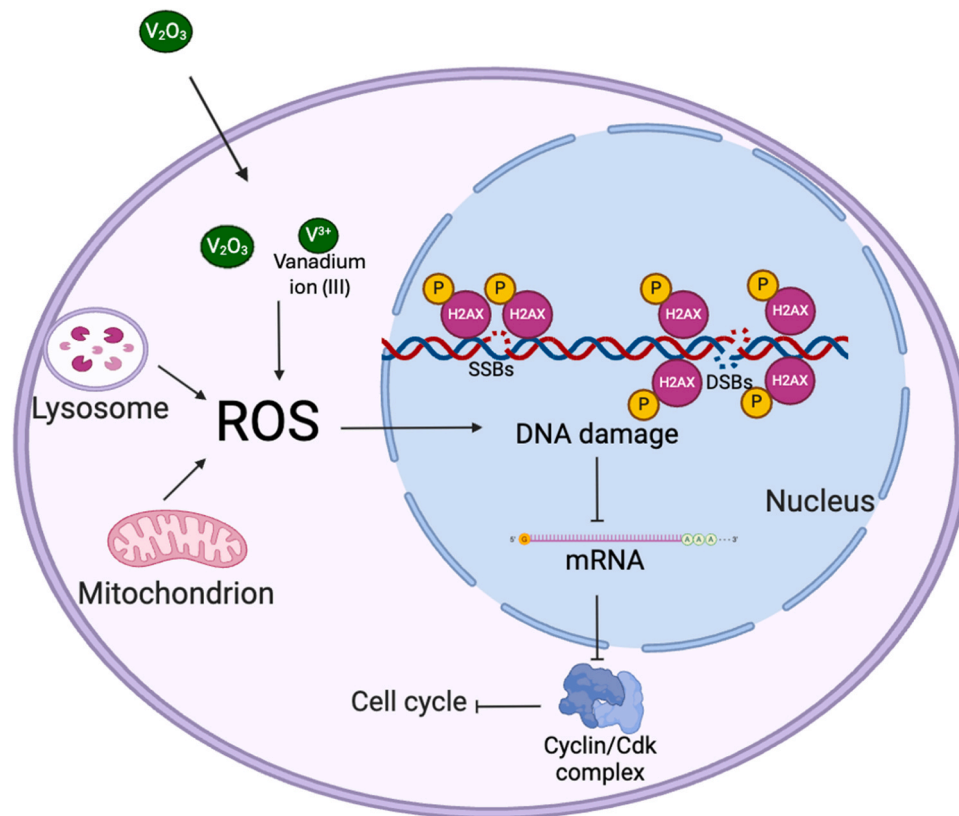
Fig. 6. Mode of action of V_2O_3. Within cells, V_2O_3 can exist as a compound or ion, and its presence modifies the structure or function of biomolecules, including the phospholipids of lysosomes and mitochondria. This modification leads to the release of their contents and an increase in ROS. H_2O_2 reacts with V^{3+} to produce $\cdot OH$, contributing to DNA damage. In this case, either ROS or vanadium in the form of a cation or compound promotes single-strand breaks (SSBs) and double-strand breaks (DSBs) in DNA, as demonstrated by H2AX phosphorylation. This process leads to cell cycle arrest by decreasing the gene expression of mRNAs and the protein expression of cyclins and CDKs.

not statistically significant, physiological delays in the transition from G_1 to S were observed, which may be related to the decrease in the expression of proteins that control the progression from one phase to the next. Previous reports support our results, in which V salts have been found to induce delays in the G_1/S transition, in S, and in G_2/M in different human cell lines, such as C141, MCF7, EC109, and AsPC-1 [30, 38–41].

3.3. Protein and mRNA expression levels

Data on protein expression levels revealed that the exposure of lymphocytes to V_2O_3 decreases the relative intensities of cyclins and CDKs. In relation to cyclins, differences were observed at a concentration of 16 µg/mL for cyclin D and at 8 and 16 µg/mL vanadium(III) for cyclin E, whereas for CDK2 (2 and 16 µg/mL) and CDK4 (2, 8 and 16 µg/mL), a decrease was observed at various concentrations (Fig. 2).

In contrast, the mRNA expression levels of *cyclin D* remained unchanged; however, a decrease in PCR products for *cyclin E* was observed at low concentrations (2 and 4 µg/mL), and a significant decrease was observed at various concentrations for *CDK4* (8 and 16 µg/mL) and *CDK2* (2, 8 and 16 µg/mL) (Fig. 3).

Cell cycle progression depends on the association of cyclins/CDKs. The cyclin D/CDK4 complex is necessary for the cell to exit the G_0 phase, whereas the cyclin E/CDK2 complex keeps pRb phosphorylated and allows the cell to complete the G_1 phase and enter the S phase [42]. In this study, the mRNA and protein expression levels of cyclin D, cyclin E, CDK2 and CDK4 decreased upon administration of V_2O_3; as a result, the cycle is momentarily arrested by lymphocytes, as the protein expression levels needed to form cyclin/CDK complexes are not reached.

V compounds have been shown to modify the expression levels of some RNAs [43], as well as cyclin and CDK proteins involved in cell cycle regulation [12,31,41,44]. V compounds have been shown to inhibit mRNA synthesis by reacting with nucleotides; in addition, these compounds activate protein phosphatases, kinases, or enzymes involved in the degradation of these polymers [45–47], which can subsequently lead to decreased expression of RNAs as gene products. Notably, the delay we observed may also be related to vanadium(III)-induced DNA damage, as cells that incur damage stop their cycle to repair DNA lesions.

3.4. DNA damage sensor protein γH2AX

With respect to the results obtained for the expression levels of γH2AX, a concentration-related increase was observed, with significant differences at concentrations of 8 and 16 µg/mL V_2O_3 (Fig. 4). γH2AX is a sensor of the DNA damage response and is indicative of double-strand breaks.

Our results show that the relative intensity of γH2AX increases. V_2O_3 induces single-strand breaks in DNA in peripheral blood leukocytes *in vitro* (1, 2, 4 or 8 µg/mL) [18] and chromosomal damage in *in vivo* experimental models [16,19], effects that have been observed with other V compounds (VCl$_3$, V_2O_4 and V_2O_5) [19,20,30,48]. Double-strand breaks in DNA are the most damaging effects to the cell because they are related to the formation of structural chromosomal aberrations [16,19], and vanadium(IV) has been demonstrated to induce this type of damage in human lymphocytes [18,37]. V_2O_3 treatment induces H2AX phosphorylation, revealing that this chemical species can induce double-chain injury, directly or indirectly (by intracellularly changing the oxidation state from III to IV).

γH2AX regulates repair pathways such as p53, which is responsible

for cell cycle arrest, among other functions; however, V_2O_3 does not modify p53 expression levels and does modify H2AX phosphorylation. Therefore, this alternative pathway may be responsible for the cell cycle delays observed in response to V_2O_3 treatment.

4. ROS

The induction of DHR oxidation was obtained by FSC/SSC dot plots, in which V_2O_3 treatment increased the fluorescence intensity at all concentrations, with significant differences at 2 (p < 0.01) and 4 μg/mL (p < 0.01) (Fig. 5). Although significant differences were not observed for some concentrations (for 8 and 16 μg/mL, they are at the limit of significance), the increase in these concentrations was at least 0.6 times greater than that of the control; therefore, this increase is important enough to discuss.

In addition, vanadium(III) oxide in lymphocyte cultures increases oxidative stress. DNA damage is linked to ROS, and V^V has been shown to promote the production of H_2O_2 [32,49] and V^{III} the formation of radicals, such as ·OH [50–52], which can lead to the oxidation of nitrogenous bases. As previously determined, when multiple lesions occur continuously on both strands of DNA, double-strand breaks can occur in this molecule [52,53]. Although increased H_2O_2 was observed in this work, H_2O_2 cannot directly damage DNA; the products of H_2O_2 are the causative agents, such as ·OH, which may be generated through the reaction of H_2O_2 with V_2O_3 ($V^{III} + H_2O_2 \rightarrow VO^{2+} + ·OH + H^+$ or $2\,V^{III} + H_2O_2 \rightarrow 2VO^{2+} + 2\,H^+$). In this reaction, VO^{2+} (V^{IV}) can enter the redox, Fenton or Haber-Weiss reactions and increase the effects [3, 50,54,55].

Finally, in this work, we found that V_2O_3 does not affect cell viability; however, it delays the cell cycle in the G1-S phase. This delay is associated with a decrease in the mRNA levels of cyclins/CDKs, as well as their protein levels, in addition to causing intracellular oxidative stress, which may cause DNA double-strand damage and H2AX phosphorylation (Fig. 6). These effects may explain the induction of chromosome damage observed in other experimental models. Further studies are needed to specify the type of DNA damage, elucidate the pathway that detects DNA damage, and identify the repair mechanisms induced by V_2O_3.

Funding

CRediT authorship contribution statement

Juan José Rodríguez: Writing – review & editing, Writing – original draft, Project administration, Investigation, Funding acquisition, Formal analysis, Data curation, Conceptualization. **Víctor Alan Alcántara-Mejía**: Writing – review & editing, Writing – original draft, Software, Resources, Methodology, Investigation, Formal analysis, Data curation. **Rodrigo Mateos-Nava**: Visualization, Validation, Supervision, Resources, Methodology, Investigation. **Lucila Álvarez-Barrera**: Visualization, Validation, Supervision, Resources, Methodology. **Edelmiro Santiago-Osorio**: Visualization, Validation, Supervision, Conceptualization. **Edmundo Bonilla-González**: Visualization, Validation, Supervision, Methodology, Formal analysis. **Mario Altamirano-Lozano**: Project administration, Methodology, Investigation, Funding acquisition, Conceptualization.

Declaration of Competing Interest

The authors declare that they have no known competing financial interests or personal relationships that could have appeared to influence the work reported in this paper

Data Availability

Data will be made available on request.

Acknowledgements

Appendix A. Supporting information

Supplementary data associated with this article can be found in the online version at doi:10.1016/j.toxrep.2024.101695.

References

1 X. Bai, L. Luo, H. Tian, S. Liu, Y. Hao, S. Zhao, S. Lin, C. Zhu, Z. Guo, Y. Lv, Atmospheric vanadium emission inventory from both anthropogenic and natural sources in China, Environ. Sci. 55 (2021) 11568–11578, https://doi.org/10.1021/acs.est.1c04766.

2 J.P. Gustafsson, Vanadium geochemistry in the biogeosphere –speciation, solid-solution interactions, and ecotoxicity, Appl. Geochem. 102 (2019) 1–25, https://doi.org/10.1016/j.apgeochem.2018.12.027.

3 Ścibior A, Kurus J, Vanadium and oxidative stress markers - *in vivo* model: a review, Curr Med Chem 26 (2019) 5456–5500, https://doi.org/10.2174/0929867326666190108112255.

4 J.A. Wiklund, J.L. Kirk, D.C. Muir, A. Gleason, J. Carrier, F. Yang, Atmospheric trace metal deposition to remote Northwest Ontario, Canada: anthropogenic fluxes and inventories from 1860 to 2010, Sci. Total Environ. 749 (2020) 1–20, https://doi.org/10.1016/j.scitotenv.2020.142276.

5 M.P. Pavageau, A. Morin, F. Seby, C. Guimon, E. Krupp, C. Pécheyran, J. Poulleau, O. F. Donard, Partitioning of metal species during an enriched fuel combustion experiment. speciation in the gaseous and particulate phases, Environ. Sci. Technol. 38 (2004) 2252–2263, https://doi.org/10.1021/es034408i.

6 I. Mjejri, A. Rougier, M. Gaudon, Low-cost and facile synthesis of the vanadium oxides V_2O_3, VO_2, and V_2O_5 and their magnetic, thermochromic and electrochromic properties, Inorg. Chem. 56 (2017) 1734–1741, https://doi.org/10.1021/acs.inorgchem.6b02880.

7 J. Martin, K. Schafner, T. Turek, Preparation of electrolyte for vanadium redox-flow batteries based on vanadium pentoxide, Energy Technol. 8 (9) (2020) 1–10, https://doi.org/10.1002/ente.202000522.

8 P. Hu, P. Hu, T.D. Vu, M. Li, S. Wang, Y. Ke, X. Zheng, L. Mai, Y. Long, Vanadium oxide: phase diagrams, structures, synthesis, and applications, Chem. Rev. 123 (2023) 4353–4415, https://doi.org/10.1021/acs.chemrev.2c00546.

9 F.L. Assem, L.S. Levy, Inhalation Toxicity of Vanadium, in: H. Michibata (Ed.), Vanadium, Springer, Dordrecht, 2012, pp. 209–224, https://doi.org/10.1007/978-94-007-0913-3.

10 T.I. Fortoul, M. Rojas-Lemus, V. Rodriguez-Lara, A. Gonzalez-Villalva, M. Ustarroz-Cano, G. Cano-Gutierrez, M. Altamirano-Lozano, Overview of environmental and occupational vanadium exposure and associated health outcomes: an article based on a presentation at the 8th International Symposium on Vanadium Chemistry, Biological Chemistry, and Toxicology, Washington DC, August 15–18, 2012, J. Immunotoxicol. 11 (2014) 13–18, https://doi.org/10.3109/1547691X.2013.789940.

11 M.A. Altamirano-Lozano, L. Alvarez-Barrera, R.A. Mateos-Nava, T.I. Fortoul, J. J. Rodriguez-Mercado, Potential for genotoxic and reprotoxic effects of vanadium compounds due to occupational and environmental exposures: an article based on a presentation at the 8th International Symposium on Vanadium Chemistry, Biological Chemistry, and Toxicology, Washington DC, August 15–18, 2012, J. Immunotoxicol. 11 (2014) 19–27, https://doi.org/10.3109/1547691X.2013.791734.

12 R.A. Mateos-Nava, J.J. Rodríguez-Mercado, L. Álvarez-Barrera, M.C. García-Rodríguez, M.A. Altamirano-Lozano, Vanadium oxides modify the expression levels of the p21, p53, and Cdc25C proteins in human lymphocytes treated in vitro, Environ. Toxicol. 36 (8) (2021) 1536–1543, https://doi.org/10.1002/tox.23150.

13 E. Montiel-Flores, O.A. Mejía-García, J.L. Ordoñez-Librado, A.L. Gutierrez-Valdez, J. Espinosa-Villanueva, C. Dorado Martínez, L. Reynoso-Erazo, R. Tron-Alvarez, V. Rodríguez-Lara, M.R. Avila-Costa, Alzheimer-like cell death after vanadium pentoxide inhalation, 1–5, Heliyon 7 (2021) https://doi.org/10.1016/j.heliyon.2021.e07856.

14 N. López-Valdez, M. Rojas-Lemus, M.P. Bizarro-Nevares, A.E. González-Villalva, M. L. Ustarroz-Cano, B. Casarrubias-Tabarez, G. Guerrero-Palomo, M.E. Cervantes-Valencia, N. Rivera-Fernández, T.I. Fortoul, Sex differences in vanadium inhalation effects in non-ciliated bronchiolar cells, Histol. Histopathol. 38 (2023) 765–777.

15 L. Álvarez-Barrera, J.J. Rodríguez-Mercado, R.A. Mateos-Nava, N.A. Ocampo-Aguilera, M.A. Altamirano-Lozano, Vanadium (IV) oxide affects embryonic development in mice, Environ. Toxicol. 37 (2022) 1587–1596, https://doi.org/10.1002/tox.23508.

16 L. Álvarez-Barrera, J.J. Rodríguez-Mercado, R.A. Mateos-Nava, A. Acosta-San Juan, M.A. Altamirano-Lozano, Cytogenetic damage by vanadium (IV) and vanadium (III)

on the bone marrow of mice, Drug Chem. Toxicol. 5 (2023) 1–8, https://doi.org/10.1080/01480545.2023.2263669.

17 J.J. Rodríguez-Mercado, L. Álvarez-Barrera, M.A. Altamirano-Lozano, Chromosomal damage induced by vanadium oxides in human peripheral lymphocytes, Drug Chem. Toxicol. 33 (2010) 97–102, https://doi.org/10.3109/01480540903176602.

18 J.J. Rodríguez-Mercado, R.A. Mateos-Nava, M.A. Altamirano-Lozano, DNA damage induction in human cells exposed to vanadium oxides *in vitro*, Toxicol. Vitr. 25 (2011) 1996–2002, https://doi.org/10.1016/j.tiv.2011.07.009.

19 J. Owusu-Yaw, M.D. Cohen, S.Y. Fernando, C.I. Wei, An assessment of the genotoxicity of vanadium, Toxicol. Lett. 50 (1990) 327–336, https://doi.org/10.1016/0378-4274(90)90026-i.

20 R.A. Mateos-Nava, J.J. Rodríguez-Mercado, M.A. Altamirano-Lozano, Premature chromatid separation and altered proliferation of human leukocytes treated with vanadium (III) oxide, Drug. Chem. Toxicol. 40 (2017) 457–462, https://doi.org/10.1080/01480545.2016.1260582.

21 A. Ciccia, S.J. Elledge, The DNA damage response: making it safe to play with knives, Mol. Cell 40 (2010) 179–204, https://doi.org/10.1016/j.molcel.2010.09.019.

22 T. Tanaka, X. Huang, H.D. Halicka, H. Zhao, F. Traganos, A.P. Albino, W. Dai, Z. Darzynkiewicz, Cytometry of ATM activation and histone H2AX phosphorylation to estimate extent of DNA damage induced by exogenous agents, J. Int Soc. Anal. Cytol. 71 (2007) 648–661, https://doi.org/10.1002/cyto.a.20426.

23 A. Maréchal, L. Zou, DNA damage sensing by the ATM and ATR kinases, Cold Spring Harb. Perspect. Biol. 5 (2013) 1–18, https://doi.org/10.1101/cshperspect.a012716.

24 A. Meier, H. Fiegler, P. Munoz, P. Ellis, D. Rigler, C. Langford, M.A. Blasco, N. Carter, S.P. Jackson, Spreading of mammalian DNA-damage response factors studied by ChIP-chip at damaged telomeres, EMBO J. 26 (2007) 2707–2718, https://doi.org/10.1038/sj.emboj.7601719.

25 V. Savic, B. Yin, N.L. Maas, A.L. Bredemeyer, A.C. Carpenter, B.A. Helmink, K. S. Yang-Lott, B.P. Sleckman, C.H. Bassing, Formation of dynamic g- H2AX domains along broken DNA strands is distinctly regulated by ATM and MDC1 and dependent upon H2AX densities in chromatin, Mol. Cell 34 (2009) 298–310, https://doi.org/10.1016/j.molcel.2009.04.012.

26 F. Mattiroli, J.H. Vissers, W.J. van Dijk, P. Ikpa, E. Citterio, W. Vermeulen, J. A. Marteijn, T.K. Sixma, RNF168 ubiquitinates K13-15 on H2A/H2AX to drive DNA damage signaling, Cell 150 (2012) 1182–1195, https://doi.org/10.1016/j.cell.2012.08.005.

27 M. Meerang, D. Ritz, S. Paliwal, Z. Garajova, M. Bosshard, N. Mailand, P. Janscak, U. Hubscher, H. Meyer, K. Ramadan, The ubiquitin-selective segregase VCP/p97 orchestrates the response to DNA double-strand breaks, Nat. Cell Biol. 13 (2011) 1376–1382, https://doi.org/10.1038/ncb2367.

28 A. Hafner, M.L. Bulyk, A. Jambhekar, G. Lahav, The multiple mechanisms that regulate p53 activity and cell fate, Nat. Rev. Mol. Cell Biol. 20 (2019) 199–210, https://doi.org/10.1038/s41580-019-0110-x.

29 A. Levina, P.A. Lay, Stabilities and biological activities of vanadium drugs: what is the nature of the active species? Chem. Asian J. 12 (2017) 1692–1699, https://doi.org/10.1002/asia.201700463.

30 A. Levina, P.A. Lay, Vanadium (V/IV)–transferrin binding disrupts the transferrin cycle and reduces vanadium uptake and antiproliferative activity in human lung cancer cells, Inorg. Chem. 59 (2020) 16143–16153, https://doi.org/10.1021/acs.inorgchem.0c00926.

31 A. Levina, D.C. Crans, P.A. Lay, Speciation of metal drugs, supplements and toxins in media and bodily fluids controls in vitro activities, Coord. Chem. Rev. 352 (2017) 473–498, https://doi.org/10.1016/j.ccr.2017.01.002.

32 H.A. Ngwa, A. Kanthasamy, V. Anantharam, C. Song, T. Witte, R. Houk, A. G. Kanthasamy, Vanadium induces dopaminergic neurotoxicity via protein kinase Cdelta dependent oxidative signaling mechanisms: Relevance to etiopathogenesis of Parkinson's disease, Toxicol. Appl. Pharma 240 (2009) 273–285, https://doi.org/10.1016/j.taap.2009.07.025.

33 E. Rojas, M. Valverde, L.A. Herrera, M. Altamirano-Lozano, P. Ostrosky-Wegman, Genotoxicity of vanadium pentoxide evaluate by the single cell gel electrophoresis assay in human lymphocytes, Mutat. Res 359 (1996) 77–84, https://doi.org/10.1016/s0165-1161(96)90254-x.

34 R.S. Ray, B. Rana, B. Swami, V. Venu, M. Chatterjee, Vanadium mediated apoptosis and cell cycle arrest in MCF7 cell line, Chem. Biol. Inter. 163 (2006) 239–247, https://doi.org/10.1016/j.cbi.2006.08.006.

35 Y. Fu, Q. Wang, X.G. Yang, X.D. Yang, K. Wang, Vanadyl bisacetylacetonate induced G1/S cell cycle arrest via high-intensity ERK phosphorylation in HepG2 cells, J. Biol. Inorg. Chem. 13 (2008) 1001–1009, https://doi.org/10.1007/s00775-008-0387-2.

36 E. Roldán, M. Altamirano, Chromosomal aberrations, sister chromatid exchanges, cell-cycle kinetics and satellite association in human lymphocytes culture exposed to vanadium pentoxide, Mutat. Res 245 (1990) 61–65, https://doi.org/10.1016/0165-7992(90)90001-z.

37 J.J. Rodríguez-Mercado, E. Roldán-Reyes, M. Altamirano-Lozano, Genotoxic effects of vanadium (IV) in human peripheral blood cells, Toxicol. Lett. 144 (2003) 359–369, https://doi.org/10.1016/s0378-4274(03)00255-8.

38 Z. Zhang, C. Huang, J. Li, X. Shi, Vanadate-induce cell growth arrest is p53-dependent through activation of p21 in C141 cells, J. Inorg. Biochem 89 (2002) 142–148, https://doi.org/10.1016/s0162-0134(01)00409-3.

39 Z. Zhang, N. Gao, H. He, C. Huang, J. Luo, X. Shi, Vanadate active Akt and promoted S phase entry, Mol. Cell Biochem 255 (2004) 2227–2237, https://doi.org/10.1023/b:mcbi.0000007278.27936.8b.

40 J.X. Wu, Y.H. Hong, X.G. Yang, Bis(acetylacetonato)-oxidovanadium(IV) and sodium metavanadate inhibit cell proliferation via ROS-induced sustained MAPK/ERK activation but with elevated AKT activity in human pancreatic cancer AsPC-1 cells, J. Biol. Inorg. Chem. 8 (2016) 919–929, https://doi.org/10.1007/s00775-016-1389-0.

41 J. Yang, Z. Zhang, S. Jiang, M. Zhang, J. Lu, L. Huang, T. Zhang, K. Gong, S. Yan, Z. Yang, G. Shao, Vanadate-induced antiproliferative and apoptotic response in esophageal squamous carcinoma cell line EC109, J. Toxicol. Environ. Health 79 (2016) 864–868, https://doi.org/10.1080/15287394.2016.1193115.

42 V.A. Blomen, J. Boonstra, Cell fate determination during G_1 phase progression, Cell Mol. Life Sci. 64 (2007) 3084–3104, https://doi.org/10.1007/s00018-007-7271-z.

43 J.L. Ingram, A. Antao-Menezes, E.A. Turpin, D.G. Wallace, J.B. Mangum, L.J. Pluta, R.S. Thomas, J.C. Bonner, Genomic analysis of human lung fibroblasts exposed to vanadium pentoxide to identify candidate genes for occupational bronchitis, Resp. Res. 8 (1) (2007) 34, https://doi.org/10.1186/1465-9921-8-34.

44 W.S. Xi, J.B. Li, Y.Y. Liu, H. Wu, A. Cao, H. Wang, Cytotoxicity and genotoxicity of low-dose vanadium dioxide nanoparticles to lung cells following long-term exposure, Toxicology 459 (2021) 1528–1559, https://doi.org/10.1016/j.tox.2021.152859.

45 I.G. Macara, Vanadium an element in search of a role, TIBS 5 (1980) 92–94, https://doi.org/10.14670/HH-18-566.

46 P. Williams, S. Etcheverry, E. Baran, Über die Wechselwirkung des Vanadyl(IV)-Kations mit Nucleobasen / Interaction of the Vanadyl(IV) Cation with Nucleic Bases, Z. F. üR. Naturforsch. B 48 (1993) 1845–1847, https://doi.org/10.1515/znb-1993-1226.

47 P.A.M. Williams, S.B. Etcheverry, E.J. Baran, A spectrophotometric study of the interaction of VO^{2+} with cytosine in nucleotides, J. Inorg. Biochem. 1 (1996) 285–289, https://doi.org/10.1016/0162-0134(94)00083-2.

48 M. Caicedo, J.J. Jacobs, A. Reddy, N.J. Hallab, Analysis of metal ion- induced DNA damage, apoptosis, and necrosis in human (Jurkat) T-cells demonstrates Ni^{2+} and V^{3+} are more toxic than other metals: Al^{3+}, Be^{2+}, Co^{2+}, Cr^{3+}, Cu^{2+}, Fe^{3+}, Mo^{5+}, Nb^{5+}, Zr^{2+}, J. Biomed. Mater. Res A 86 (2007) 905–913, https://doi.org/10.1002/jbm.a.31789.

49 I. Zwolak, Protective effects of dietary antioxidants against vanadium-induced toxicity: a review, Oxid. Med. Cell Longev. 2020 (2020) 1490316, https://doi.org/10.1023/b:mcbi.0000007278.27936.8b.

50 G. Du, J.H. Espenson, Oxidation of vanadium(III) by hydrogen peroxide and the oxomonoperoxo vanadium(V) ion in acidic solutions: a kinetics and simulation study, Inorg. Chem. 44 (2005) 5514–5522, https://doi.org/10.1021/ic050502j.

51 H. Fickl, A.J. Theron, H. Grimmer, J. Oommen, G.J. Ramafi, H.C. Steel, S.S. Visser, R. Anderson, Vanadium promotes hydroxyl radical formation by activated human neutrophils, Free Radic. Biol. Med 40 (2006) 146–155, https://doi.org/10.1016/j.freeradbiomed.2005.09.019.

52 D.R. Lloyd, P.L. Carmichael, D.H. Phillips, Comparison of the formation of 8-hydroxy-2 '-deoxyguanosine and single-and double-strand breaks in DNA mediated by fenton reactions, Chem. Res Toxicol. 11 (1998) 420–427, https://doi.org/10.1021/tx970156l.

53 V. Sharma, L.B. Collins, T.H. Chen, N. Herr, S. Takeda, W. Sun, J. Nakamura, Oxidative stress at low levels can induce clustered DNA lesions leading to NHEJ mediated mutations, Oncotarget 7 (2016) 25377.

54 L.A. Soriano-Agueda, C. Ortega-Moo, J. Garza, J.A. Guevara-Garcia, R. Vargas, Formation of reactive oxygen species by vanadium complexes, Comput. Theor. Chem. 1077 (2016) 99–105, https://doi.org/10.1016/j.comptc.2015.11.002.

55 X. He, Z.R. Jarrell, Y. Liang, M.R. Smith, M.L. Or, L. Marts, D.P. Jones, Vanadium pentoxide induced oxidative stress and cellular senescence in human lung fibroblasts, Redox Biol. 55 (2022) 1–12, https://doi.org/10.1016/j.redox.2022.102409.